COMPACT MULTI-USER WIDEBAND MIMO SYSTEM USING MULTIPLE-MODE ANTENNAS

A Thesis by

Amitav Mukherjee

Bachelor of Science, University of Kansas, 2005

Submitted to the Department of Electrical Engineering
and the faculty of the Graduate School of
Wichita State University
in partial fulfillment of
the requirements for the degree of
Master of Science

May 2007

COMPACT MULTI-USER WIDEBAND MIMO SYSTEM USING MULTIPLE-MODE ANTENNAS

I have examined the final copy of this thesis for form and content, and recommend that it be accepted in partial fulfillment of the requirement for the degree of Master of Science with a major in Electrical Engineering.

_____

Hyuck M. Kwon, Committee Chair

We have read this thesis
and recommend its acceptance:

_____

John Watkins, Committee Member

_____

Krishna Krishnan, Committee Member

To my parents and the brave soldiers of the Jammu & Kashmir Rifles regiment of the Indian Army

It is better to do one’s own duty, however defective it may be, than to follow the duty of another, however well one may perform it. He who does his duty as his own nature reveals it, never sins. Perseverance in seeking to gain the knowledge of the Supreme Spirit, and perception of the gain that comes from knowledge of the truth: This is called knowledge : all that is contrary to this is ignorance.
-(Bhagavad Gita 13:11)

ACKNOWLEDGEMENTS

The list of people who have made this work possible is at times long or short depending upon my perspective. At any rate, all due credit must be given to Dr. Hyuck M. Kwon for his patience and insightful guidance over the course of the past three semesters. I am grateful to my committee members Dr. Watkins and Dr. Krishnan for their support. This section would be incomplete without mentioning my colleagues in the Wireless Communications Group who have unwittingly spurred along this thesis in various ways. Last but not the least, my being in this position would not have been possible but for three unique individuals who bear the same last name as me, and who have tolerated me since the day I was born.

ABSTRACT

A complete multiple-input multiple-output (MIMO) communication system with orthogonal frequency-division multiplexing (OFDM) based on multiple excitation modes for a single circular microstrip antenna is introduced. Traditional diversity techniques such as spatial diversity by means of a linear antenna array or polarization diversity by means of a cross-polarized antenna array may prove to be unsuitable in the case of severe restrictions on antenna size and spacing. A single microstrip antenna employing multiple modes is shown to be comparable to conventional antenna arrays at a much lower cost in terms of size and spacing in an urban micro-cell setting as defined by the Third-Generation Partnership Project (3GPP) standards body. The throughput performance and signal detection of multimode antennas in flat and frequency-selective fading environments is examined subsequently.
Mathematical expressions for the increase in capacity and diversity using an array of multimode antennas are derived thereafter. Finally, a novel space-pattern diversity array is analyzed to determine theoretical limits of capacity and diversity gain over traditional spatial MIMO diversity.

Table of Contents

List of Figures

ABBREVIATIONS AND SYMBOLS

a	Antenna radius
k_f	free-space propagation constant
λ	Wavelength
ρ_e	Envelope correlation
θ	Elevation angle
φ	Azimuthal angle
d	Antenna array element separation
ε_r	Relative Permittivity
τ_{RMS}	RMS Delay Spread
J_n	Bessel function of order n
B	Signal Bandwidth
ϵ	Complex domain
3G	Third Generation
3GPP	Third Generation Partnership Project
AoA	Angle of Arrival
AoD	Angle of Departure
AS	Angle Spread
AWGN	Additive White Gaussian Noise
BER	Bit Error Rate
BPSK	Binary Phase Shift Keying
BS/MS	Base Station/Mobile Station
COST	European Cooperation in the field of Scientific and Technical Research

CSIT	Channel State Information at Transmitter
dB	decibels
DS	Delay Spread
ETSI	European Telecommunications Standards Institute
GSM	Global System for Mobile Communications
i.i.d	independent and identically-distributed
ISI	Inter-symbol Interference
MEA	Multimode Element Array
LOS	Line-of-Sight
MIMO	Multiple-Input Multiple-Output
MMSE	Minimum Mean-square Error
NLOS	Non Line-of-Sight
OFDM	Orthogonal Frequency Division Multiplexing
PAS	Power Azimuth Spectrum
PEP	Pairwise Error Probability
PDP	Power Delay Profile
PL	Path Loss
QAM	Quadrature Amplitude Modulation
SCM	Spatial Channel Model
SDMA	Spatial Division Multiple Access
SNR	Signal-to-Noise Ratio
SPC	Successive Pattern Cancellation
TDMA	Time Division Multiple Access

TEM	Transverse Electric and Magnetic
TM	Transverse Magnetic
ULA	Uniform Linear Array
XPD	Cross-polarization discrimination
ZF	Zero-Forcing

Chapter 1

INTRODUCTION

The field of wireless communications has been expanding at an overwhelming rate over the past decade. Current theoretical research is focused on studying the interaction between multiple users in a wireless environment, where each user employs multiple antennas to achieve maximal data rates. This is prompted by the well-known theoretical results on the increase in data rates for multiple-input multiple-output (MIMO) systems presented in [1], [2]. MIMO systems enhance capacity by exploiting spatial diversity without requiring additional bandwidth, thereby greatly increasing spectral i.e. bandwidth efficiency as seen in Fig 1. For this reason, the MIMO system architecture has been adopted for upcoming cellular communications standards such as Third Generation (3G) systems. The traditional form of MIMO space diversity consists of multiple antennas physically separated by an order of wavelengths λ at both transmitter and receiver.

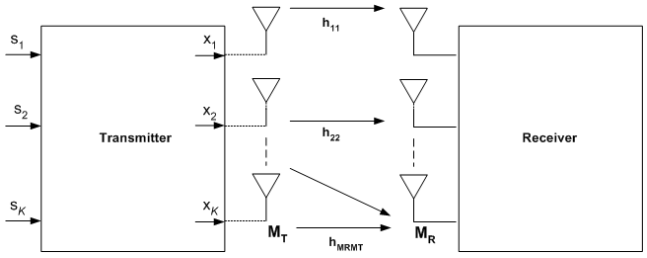

Figure 1.1: MIMO System showing spatial diversity between the transmitter and receiver

1.1 Motivation

However, the traditional MIMO approach of using a linear antenna array with multiple elements separated by half-wavelength or more poses various implementation problems. The diversity gain achieved is inversely proportional to the level of received signal correlation ρ_e. Clarke [3] derived the following relationship between ρ_e and antenna separation d, with J_0 being the zero-order Bessel function:

$$\rho_e = J_0^2(\frac{2\pi d}{\lambda}) \tag{1.1.1}$$

Fitting several antennas onto a small Mobile Station (MS) handset with sufficient element separation to achieve $\rho_e \leqslant 0.5$ is a formidable challenge due to the severe restrictions on space and aesthetics. Furthermore, it is complicated to calibrate and maintain antenna arrays with many antenna elements. Alternative diversity solutions such as polarization diversity also suffer from similar impediments, though to a lesser degree. A diversity mechanism based upon the different far-field radiation patterns of higher-order antenna modes is an alternative which is considered in this thesis to resolve the problems stated above. Diversity gain in this case can be explained by the fact that different antenna patterns receive different sets of multipath waves [5].

In addition to the form factor of antenna arrays, another key aspect of this thesis is the choice of channel propagation model. The vast majority of technical papers on MIMO systems use highly simplistic channel models such as a purely i.i.d Rayleigh model, or simple ray-tracing models such as one-ring or two-ring. These models generate theoretical capacity predictions which have been found to be overly optimistic when compared to experimental MIMO measurements. This thesis therefore carries out analysis of antenna array performance using the Third Generation Partnership Project (3GPP) Spatial Channel Model (SCM), which has been developed based on experimental campaigns carried out over the course of the past 20 years.

1.2 Background and Previous Work

The notion of using higher-order antenna modes for wireless communications is generally considered to have first been proposed in [4]. The case of circular microstrip antennas employing higher-order modes was examined in detail by Vaughan [12] with emphasis on the electromagnetic theory aspects. Demmerle and Wiesbeck implemented this form of pattern diversity using a single biconical [8] and a single spiral [9] antenna element and showed that Spatial Division Multiple Access (SDMA) was achievable. Svantesson [10] extended multimode antennas (biconical and microstrip patch) to include MIMO applications and demonstrated that multimode antennas offer characteristics similar to those of an uniform linear array (ULA) by using only a single antenna element. However, [10] used a rough approximation of the far-field patterns of a circular microstrip antenna given in [12] by neglecting the azimuthal component, in addition to using a simplistic one-ring channel model. The case of a two-element array of collocated multimode circular patch antennas was examined in [11], but considered only one higher-order mode generation at a time on each element. The modeled environment was the indoor clustered 802.11 model where due to collocation, spatial diversity was also not a factor.

Additionally, possible MIMO applications are considered in [10], [9] and [11] from the perspective of achievable receive diversity gain without any emphasis on the problem of detection and separation of user data streams at the receiver. The channel model used in [10] and many other articles on MIMO systems is a simplistic one-ring or two-ring model which provides overly optimistic channel capacity results when compared with experimental results [15], [20]. Similarly, [11] uses the Kronecker channel model which has been shown to have inaccurate mutual information and expected error performance [20]. In addition, the concept of MIMO arrays utilizing space-mode or space-frequency-mode diversity has not been proposed prior to this thesis.

1.3 Contributions

This thesis has the following novel contributions:

- Analysis and throughput comparison of multimode and conventional ULA antennas in the 3GPP urban micro-cell environment with narrowband signals.
- Analysis of signal detection and error performance of multimode antennas and proposal of detection algorithm named Successive Pattern Cancellation (SPC).
- Implementation of OFDM in multimode antennas and consequent analysis of wideband MIMO performance in a frequency-selective fading environment.
- Introduction of spatial/mode diversity arrays for wireless communication which offer additional diversity gain compared to conventional space-frequency arrays.

1.4 Thesis Organization

The current chapter has served to introduce the motivation behind this thesis and an overview of previous work in the area of multimode antennas. The remainder of this work is organized as follows.

Chapter 2 reviews the electromagnetic aspects of multimode microstrip antennas and verifies that different modes may be used to generate dissimilar far-field antenna patterns.

Chapter 3 covers commonly-used MIMO propagation models such as the one-ring and two-ring models and introduces the 3GPP urban micro-cell system model in detail.

Chapter 4 examines the problem of signal detection and demodulation at the receiver end when using multimode diversity. The motivation behind introduction of SPC is defined.

Chapter 5 proposes and analyzes MIMO arrays employing a combination of space and pattern diversity. Quantitative predictions of the increase in MIMO capacity and diversity gain for spatial-pattern diversity arrays are subsequently presented.

Chapter 6 presents simulation results for multimode capacity performance compared to conventional linear arrays in a variety of channel and array scenarios. Both narrowband and wideband MIMO system capacities are presented, followed by numerical evaluations of the bit error rate (BER) for multimode antennas with and without OFDM.

Chapter 7 offers conclusions and suggestions for future research.

Chapter 2

ELECTROMAGNETIC THEORY OF MULTIMODE ANTENNAS

The phenomenon of higher order antenna modes has been well documented in antenna-specific literature. The key idea that allows such modes to be used as individual antenna ports for MIMO systems is that different modes have differing far-field radiation patterns that are also dependent upon the azimuthal orientation.

2.1 Fundamental EM Concepts

A good starting point would be to define what is a mode and how it can be applied to multi-user communications. Various antenna modes originate as propagation modes from within the input waveguide, which necessitates a brief review of transmission line theory. Waveguides are generally useful only for signals of extremely high frequency, where the wavelength λ approaches the cross-sectional dimensions of the waveguide. Below such frequencies, waveguides are useless as electrical transmission lines. Antennas can be considered as a particular class of waveguides which radiate energy.

Waveguides may be thought of as conduits for electromagnetic energy, the waveguide itself acting as nothing more than a 'director' of the energy rather than as a signal conductor in the normal sense of the word. In a sense, all transmission lines function as conduits of electromagnetic energy when transporting pulses or high-frequency waves. However, because waveguides are single-conductor elements, the propagation of electrical energy down

a waveguide is of a very different nature than the propagation of electrical energy down a two-conductor transmission line.

All electromagnetic waves consist of electric and magnetic fields propagating in the same direction of travel, but perpendicular to each other. Along the length of a normal transmission line, both electric and magnetic fields are perpendicular (transverse) to the direction of wave travel. This is known as the principal mode, or TEM (Transverse Electric and Magnetic) mode. This mode of wave propagation can exist only where there are two conductors, and it is the dominant mode of wave propagation where the cross-sectional dimensions of the transmission line are small compared to the wavelength of the signal. When an electromagnetic wave propagates down a hollow tube, only one of the fields, either electric or magnetic, will actually be transverse to the wave's direction of travel. The other field will "loop" longitudinally to the direction of travel, but still be perpendicular to the other field. Whichever field remains transverse to the direction of travel determines whether the wave propagates in TE mode (Transverse Electric) or TM (Transverse Magnetic) mode.

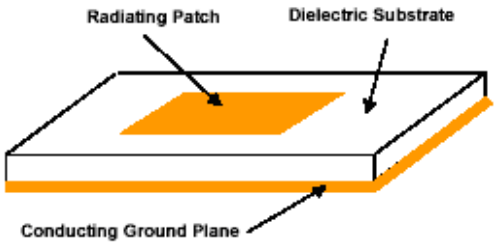

Figure 2.1: Conventional rectangular microstrip patch antenna

2.2 Multimode Microstrip Radiation Patterns

The phenomenon of higher order antenna modes has been well documented in physics and antenna-specific literature since 1950, but has not received much attention from communications engineers until the last decade. The key idea that allows such modes to be used as individual antenna ports for MIMO is that different modes have differing far-field radiation

patterns that are also dependent upon the azimuthal orientation.

The antenna structure that is considered in the remainder of this work is the microstrip or patch antenna. The author would like to emphasize that not only microstrip but almost all antenna structures such as biconical, helical, spiral and log-periodic antennas are capable of generating higher-order or multimodes. Microstrip antennas were chosen for detailed analysis since they are a commonly used class of antennas in mobile communications, as well as due to the author's prior experience in designing and fabricating such antennas.

The m^{th}-order mode far-field radiation pattern at a radial distance r for a microstrip antenna of radius a and thickness h is

$$\overrightarrow{E_m} = \frac{-e^{jkr}}{r}(\overrightarrow{\theta}\, E_{m,\theta} + \overrightarrow{\phi}\, E_{m,\phi}) \tag{2.2.1}$$

where

$$E_{m,\theta} = \frac{j^m V_m^0 k_f a}{2}(J_{m+1}(z) - J_{m-1}(z))(\cos\left[m(\phi - \phi_0\right]) \tag{2.2.2}$$

$$E_{m,\phi} = \frac{j^m V_m^0 k_f a}{2}(J_{m+1}(z) - J_{m-1}(z))(\cos\theta)(\sin\left[m(\phi - \phi_0\right])) \tag{2.2.3}$$

$$z = k_f a(\sin\theta) \tag{2.2.4}$$

$J_m(x)$ represents the second Bessel function of order m and argument x, and ϕ and θ represent the elevation and azimuthal angles respectively. In addition, ϕ_0 is the reference angle corresponding to the input feed point with peak input voltage V_m^0 for the m^{th} mode, and k_f is the free-space propagation constant (wave number).

Fig. 2.2 depicts the far-field radiation patterns for modes 1, 2, 5 and 6. The 0^{th} or fundamental mode has an isotropic radiation pattern which may be inferred from eq. 2.2.2, thereby rendering it unsuitable for the purpose of creating directional patterns. The radius of the multimode antenna is proportional to the number of modes that can be supported [24], as shown here

$$\overrightarrow{a} = \frac{\chi^{'}\lambda}{2\pi\sqrt{\epsilon_r}} \tag{2.2.5}$$

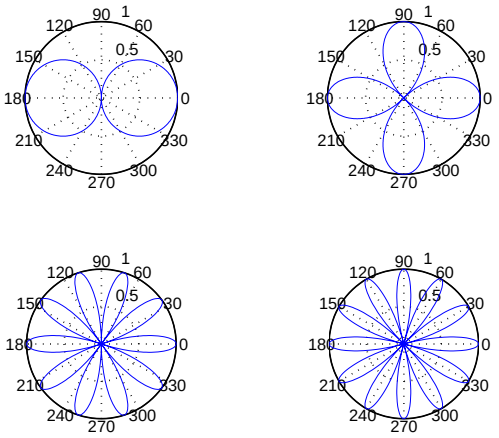

Figure 2.2: Individual far-field antenna radiation patterns for a microstrip circular antenna excited with multiple modes. (a) $m = 1$. (b) $m = 2$. (c) $m = 5$. (d) $m = 6$.

where λ is the wavelength corresponding to the system carrier frequency, ϵ_r is the dielectric constant of the patch substrate, and $\chi^{'}$ is the first zero of the derivative of Bessel function J_m. For a carrier frequency of 2 GHz and $\epsilon_r = 2.5$, 6 antenna modes may be supported by a patch radius of 12 cm. The feed geometry for exciting multiple modes on a circular microstrip antenna is given in detail in [12] and [7]. We assume coaxial feeds that are modeled as infinitesimally thin plane current sheets. In order to excite higher-order modes we have off-center multiple feeds with coordinates (α_0, β_0) where $0 < \alpha_0 < a$, and assume a single mode is excited by a single feed.

The microstrip antenna is configured such that multiple higher-order modes exist simultaneously as seen in [10]. All modes are assumed to have the same polarization; therefore polarization diversity is not included in the analysis. At any given time, the transmitted radiation pattern is determined by the number of active input feeds to the antenna. If each input feed represents an independent data stream, the maximum number of data streams that can be transmitted is obviously governed by the number of modes N_m the antenna can support. Therefore, each mode is analogous to an element of a conventional uniform linear

antenna array (ULA). Fig. 2.3 shows the net radiation patterns obtained by the simultaneous generation of multiple modes.

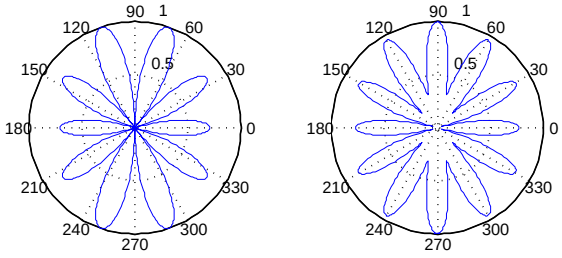

Figure 2.3: Far-field radiation patterns obtained by superimposition of multiple modes. (a) Net pattern for $m = 2$, 3 and 5. (b) Net pattern for $m = 1, 3, 4, 5$ and 6.

The advantage of using multiple antenna modes at the same time is evident: a single-mode transmission scheme as in [12] and [9] can carry only one data stream at a time, compared to multiple data streams (up to N_m) for the proposed system.

Chapter 3

URBAN MICRO-CELL PROPAGATION MODEL

The propagation environment of choice in this thesis is the urban micro-cell [34], [36]. In brief, the urban micro-cell is defined as a cell of radius less than 1 km, or in other words two neighboring base stations are separated by no more than 1 km. This is the cellular industry propagation model for urban areas with dense populations or buildings with tall profiles, such as downtown Wichita. The urban micro-cell scenario assumes that the Base Station (BS) array is at rooftop-height compared to surrounding buildings.

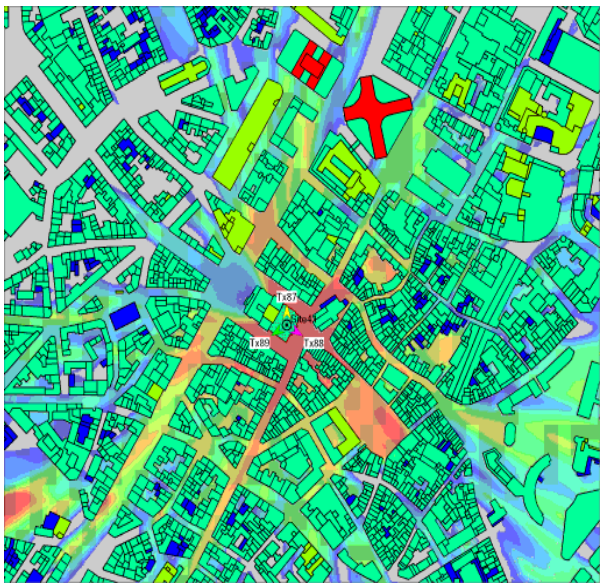

Figure 3.1: Urban micro-cell showing signal propagation and path loss in Karlsruhe, Germany. Strong signal areas are marked bright red, moderate signal strength is indicated by green, and no-signal areas are blue.

3.1 i.i.d Rayleigh Fading Channel Model

The independent and identically distributed (i.i.d.) flat Rayleigh fading channel is the simplest and the most common channel model. An i.i.d. flat Rayleigh fading MIMO channel $\mathbf{H}_w$ (also known as spatially white channel) is defined as having elements $h_{i,j}$

$$h_{i,j} = \sqrt{0.5}[\mathcal{N}(0,1) + j\mathcal{N}(0,1)] \tag{3.1.1}$$

where $\mathcal{N}(0,1)$ denotes the normal distribution with zero mean and unit variance. Fading paths are assumed to be uncorrelated with no mutual coupling between antennas.

3.2 One-Ring MIMO Channel Model

The One-Ring channel model has been described in [43], and used in [10] for multimode MIMO. In this model, the BS is assumed to be elevated, which means that there is no obstruction by local scattering while the MS is surrounded by a finite number of scatterers lying in a circular disc with uniform distribution as seen in Fig. 3.2. The scatterers are assumed to be omnidirectional re-radiating objects which reflect the plane wave directly to the receiver antenna without influencing other scatterers [21]. Only those rays that reflect once by the scatterer are considered, therefore this model is also known as the 'single-scatterer' or 'single-bounce' model.

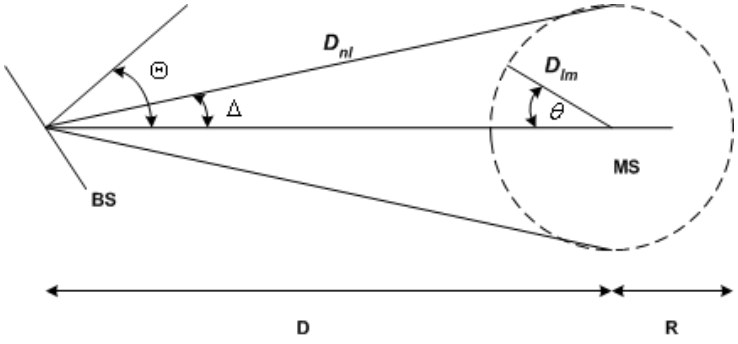

Figure 3.2: One-ring channel model showing ring of scatterers around the MS [42]

For this model, the entries of the channel matrix $\mathbf{H}$ are generated as follows. Considering a single transmission path from n^{th} transmit antenna to m^{th} receive antenna intercepted

and reflected by l^{th} scatterer, the channel gain $h_{i,j}$ is given as

$$h_{i,j} = \sqrt{\frac{1}{L}} \sum_{l=1}^{L} \left(\alpha_l e^{[-j\frac{2\pi}{\lambda}(D_{lm}+D_{nl})]} \right) \tag{3.2.1}$$

where $\alpha_l \sim \mathcal{N}(0,1)$ is the scattering coefficient due to the l^{th} scatterer ($l = 1, 2, \ldots, L$), D_{lm} is the distance between the m^{th} receive antenna and l^{th} scatterer, D_{nl} is the distance between the l^{th} scatterer and the n^{th} transmit antenna. The two-ring channel model is identical to the one-ring model with the addition of a uniformly distributed ring of scatterers around the BS itself.

3.3 3GPP Urban Micro-cell Model

The broadband spatial channel model (SCM) for MIMO [22] is chosen for analysis as it is be considered to be more realistic than the purely i.i.d Rayleigh fading [14] or the one-ring [21] and two-ring outdoor channel models. In brief, the SCM is a 2-D parameter channel model, which considers N clusters of scatterers. Each cluster corresponds to a path. There are M unresolvable sub-paths within a path ($M = 20$) for SCM).

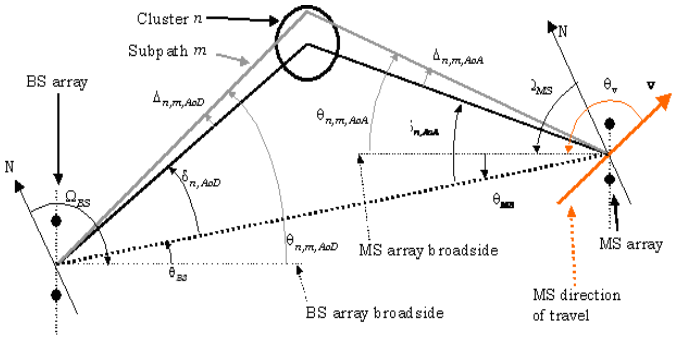

Figure 3.3: 3GPP SCM for antenna-arrays on the system downlink [22]

The microcell NLOS pathloss is based on the COST 231 Walfish-Ikegami NLOS model [31], [32] with the following parameters: BS antenna height 12.5 m, building height 12 m, building to building distance 50 m, street width 25 m, MS antenna height 1.5 m, orientation 30 deg for all paths, and selection of metropolitan center. For an S element linear BS array and a U element linear MS array, the channel coefficients for one of N multi-path

components are given by a matrix of complex amplitudes. If we denote the channel matrix for the n^{th} multi-path component ($n = 1, \ldots, N$) as $\mathbf{A}_n(t)$, then the $(u, s)^{th}$ component ($s = 1, \ldots, S; u = 1, \ldots, U$) of $\mathbf{A}_n(t)$ is denoted by $h(t)$ and written as [22]

$$h(t) = \sqrt{\frac{P_n \sigma_{SF}}{M}} \sum_{m=1}^{M} \left(\sqrt{G_{BS}(\theta_{n,m}^{AoD})} e^{j[k_f d_s \sin(\theta_{n,m}^{AoD}) + \Phi_{n,m}]} \sqrt{G_{MS}(\theta_{n,m}^{AoA})} e^{j[k_f d_u \sin(\theta_{n,m}^{AoA})]} e^{j[k_f \Psi]} \right) \tag{3.3.1}$$

where

Ψ	$\|\|v\|\| \cos(\theta_{n,m,AoA-\theta_v} t)$
σ_{SF}	is the lognormal shadow fading, applied as a bulk parameter to the n paths for a given drop.
M	is the number of sub-paths per path.
$\theta_{n,m}^{AoD}$	is the AoD for the m^{th} subpath of the n^{th} path.
$\theta_{n,m}^{AoA}$	is the AoA for the m^{th} subpath of the n^{th} path.
$G_{BS}(\theta_{n,m,AoD})$	is the BS antenna gain of each array element or mode.
$G_{MS}(\theta_{n,m,AoA})$	is the MS antenna gain of each array element or mode.
j	is the square root of -1.
d_s	is the distance (meters) to BS element s from reference ($s = 1$) antenna. For the reference antenna s = 1, $d_1 = 0$.
d_u	is the distance (meters) to MS element u from reference ($u = 1$) antenna. For the reference antenna $u = 1$, $d_1 = 0$.
$\Phi_{n,m}$	is the phase of the m^{th} subpath of the n^{th} path.
$\|\|v\|\|$	is the magnitude of the MS velocity vector.
θ_v	is the angle of the MS velocity vector.

It is evident that the 3GPP SCM is a vastly more complex modeling tool compared to the i.i.d and one-ring MIMO channel models. This conclusion is supported by the fact that the author's MATLAB implementation of the 3GPP SCM spans nearly 2000 lines of code, compared to a combined 50 lines for the i.i.d and one-ring models. The author conjectures that the complexity of the 3GPP SCM is one of the reasons why very few research papers in the last few years have used this model for capacity predictions.

Chapter 4

SIGNAL DETECTION FOR MULTIMODE MIMO ANTENNAS

4.1 Flat Fading

In this section, flat fading signifies that the modulated signal bandwidth B is much narrower than the channel coherence bandwidth. Hence, no frequency-division multiplexing is used because the component channel frequency response is relatively constant over the signal bandwidth B. Using the parameters from the previous chapter for the generation of $N_m \times N_m$, i.e., $U \times S$ channel coefficient matrix $\mathbf{H}$ which is analogous to $\mathbf{A}_n(t)$ from the previous chapter, the received signal vector of our multimode MIMO system with N_m modes may be modeled as

$$\mathbf{r_k} = \sqrt{\frac{SNR}{N_m}}\mathbf{H}\mathbf{s}_k + \mathbf{n}_k \tag{4.1.1}$$

where SNR is the signal-to-noise ratio, k is the symbol index, $\mathbf{r} \in \mathcal{C}^{N_m \times 1}$ is the received signal vector, $\mathbf{s} \in \mathcal{C}^{N_m \times 1}$ is the transmitted signal vector, and $\mathbf{n} \in \mathcal{C}^{N_m \times 1}$ is the complex zero-mean additive white Gaussian noise vector with covariance matrix $E[\mathbf{n}\mathbf{n}^\dagger]$, where E is the statistical expectation.

4.2 Frequency-Selective Fading

Wideband MIMO channels are usually defined by a bandwidth-delay spread product $B \times \tau_{RMS} \geqslant 0.1$, The r.m.s. delay spread τ_{RMS} is the standard deviation (or root-mean-square)

value of the delay of reflections, weighted proportional to the energy in the waves scattered by multipaths. Such wideband channels suffer from frequency-selective fading, i.e. the channel response $\mathbf{H}(\mathbf{f})$ varies over B. Orthogonal frequency division multiplexing (OFDM) has been proposed as a multi-carrier scheme to combat the effects of frequency-selective fading [42]. MIMO systems combined with OFDM have been proposed as a suitable alternative for wideband channels [41]. For the wideband transmission scenario, each mode comprises an OFDM transmitter employing N_c subcarriers (tones). The coherence bandwidth is constant over a subcarrier but varying over the entire bandwidth which characterizes a frequency-selective fading channel.

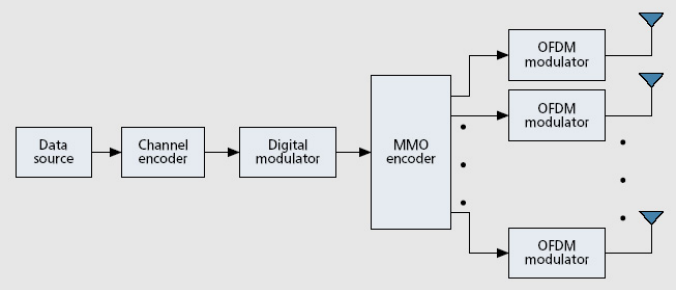

Figure 4.1: MIMO-OFDM system.

In this case, the received vector r_c on the c^{th} subcarrier can be represented as

$$\mathbf{r_c} = \sqrt{\frac{SNR}{N_m}}\mathbf{H}\mathbf{s}_c + \mathbf{n}_c \tag{4.2.1}$$

where s_c is the $N_m \times 1$ transmitted vector, n_c is additive noise with zero mean and unit variance, and H is the dimensional frequency-selective channel matrix for the cumulative N multipaths.

Table 4.1: OFDM Parameters

Data subcarriers	64
Subcarrier spacing	15 kHz
OFDM Symbol Time	64 symbol periods
Guard Interval	16 symbol periods
QAM Modulation Order	1, 2, 4, 6 or 8

We consider a maximum of $N = 6$ multipaths generated using the power delay profile

specified by the 3GPP urban micro-cell SCM [5]. Adaptive bit-loading [25] and variable-rate variable-power M-ary Quadrature Amplitude Modulation (MQAM) [26] up to 256-QAM is adopted for performance optimization.

4.3 Multimode Signal Detection

This section considers the various possible approaches to multimode signal demodulation and detection.

4.3.1 Matched Filter/Detector

Given the above representation for the received signal at the MS, we may apply techniques such as matched filter/detector or MMSE [14] for signal detection and separation. This is simplified by the assumption that the radiation patterns of all the modes used for communication are known both to the transmitter as well as receiver. Let the information bit-stream for user i at time t be denoted by $\mathbf{d}_m^i(t)$ which is selected for transmission using antenna mode m. Assuming binary phase-shift keying (BPSK) modulation, the transmitted signal for the m^{th} data stream with antenna gain $g_m(\phi)$ is

$$\mathbf{s}_m(t) = \mathbf{d}_m^i(t) g_m(\phi) \tag{4.3.1}$$

Therefore, the net transmitted signal vector $\mathbf{s}$ is a combination of all the user signals active over any given symbol period. This suggests that a simple detection methodology would be to perform a signal correlation (using inner product) between the received symbol r_k and each of the known mode patterns in parallel. As mentioned earlier, the inner product of dissimilar modes is negligible. Symbol detection may then be performed by a hard decision on the sign of the inner product with a threshold of zero.

4.3.2 Successive Pattern Cancellation (SPC)

Higher order modes present in a super-imposed transmission signal will exhibit a higher correlation with the net signal compared to lower order modes. Therefore, for enhanced

modal detection, successive interference cancellation (SIC) with regard to the multimode patterns may be applied as an additional stage after the initial matched filter banks. The matched filter values for all modes are arranged in ascending order to determine the dominant mode present. The radiation pattern corresponding to this mode is then subtracted from the received signal r and the mode detection stage is repeated to ensure that all the transmitted modes have been detected.

4.3.3 Zero-Forcing and MMSE detection

Zero-forcing equalization (ZFE) is a well-known candidate for mode detection with the inherent disadvantage of noise power enhancement [27]. Minimum mean-square error (MMSE) estimation is another candidate for linear multimode detection in both the flat-fading as well as OFDM (frequency-selective fading) scenarios. The standard MMSE expression is as follows [28]

$$G_{MMSE} = \sqrt{\frac{N_m}{E_s}} \left(\mathbf{H}^{\dagger}\mathbf{H} + \frac{N_m}{SNR}\mathbf{I}_{N_m} \right) \tag{4.3.2}$$

Chapter 5

MULTIMODE MIMO CAPACITY AND DIVERSITY

Conventional diversity approaches in wireless communications may be summarized as follows:

- Spatial diversity
- Time diversity
- Frequency diversity
- Polarization diversity
- Multiuser diversity
- Cooperative diversity

Time diversity implies that the same data is transmitted multiple times to combat channel errors [39]. Since this leads to a loss in throughput due to symbol repetition, time diversity will not be considered in this work which is focused on maximizing data rate. Polarization diversity techniques have not received as much attention as others due to the significant difference in mean signal level between co-polarized and cross-polarized branches when one polarization is transmitted [29]. Although effective, polarization diversity alone does not suffice once the number of antennas exceeds the number of orthogonal polarizations,

which is very small [30]. Hence, in large arrays polarization diversity must be combined with space diversity for effectiveness.

Until now, MIMO arrays have been restricted to those which simultaneously exploit space-frequency or space-polarization diversity. For the former case, a joint space-frequency waterfilling algorithm has been shown to be the optimal transmission strategy in the full CSIT case [38], [40]. This chapter introduces a novel MIMO array which exploits space-mode or space-frequency-mode diversity which allows waterfilling in three dimensions.

For the remainder of this chapter, we consider a single-user MIMO scenario with two different arrays: a $M \times M$ ULA of single-mode dipoles and a $P \times P$ MEA of N-multimode patch antennas as illustrated in Fig. 5. Both the ULA and the MEA are assumed to have identical element spacings of $d = \lambda$. Asymptotic bounds on the capacity and diversity gain for the MEA over the ULA are derived for theoretical understanding. Practical issues such as any increase in number of power amplifiers are not considered in this section.

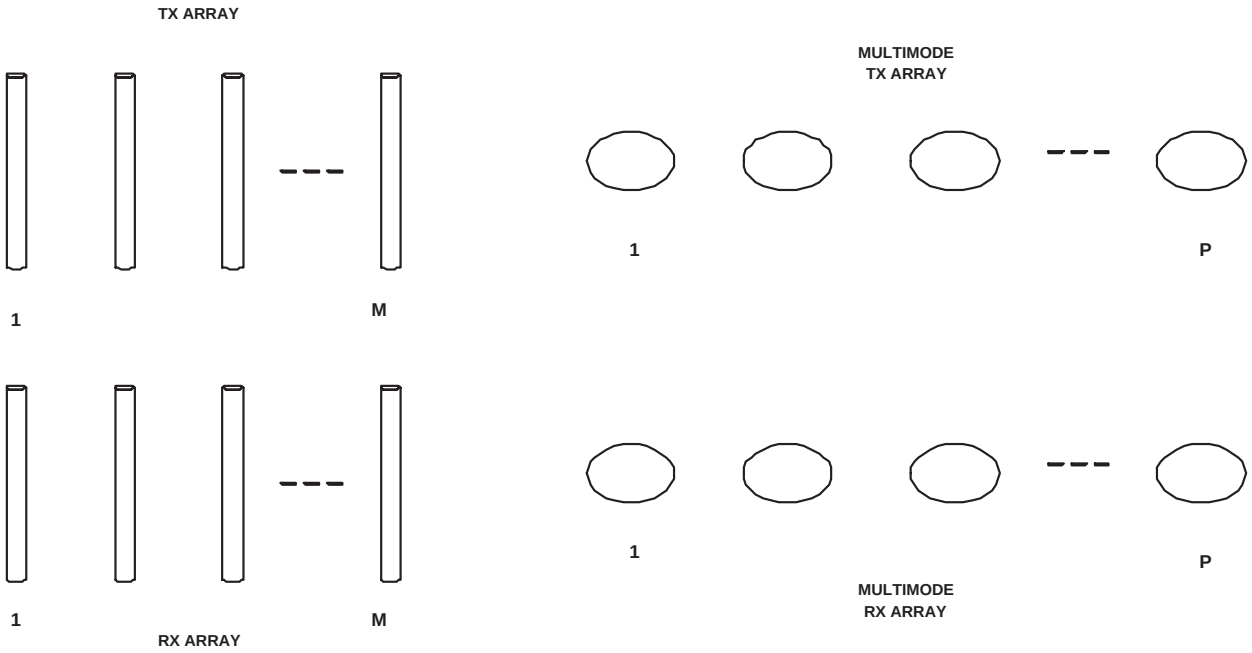

Figure 5.1: M-dipole ULA and N-mode multimode element array

It is well-known that the instantaneous channel capacity of a $M \times M$ MIMO channel with channel matrix $\mathbf{H}$ known at the receiver can be represented as [1]

$$C = \log_2 |\mathbf{I}_M + \frac{SNR}{M}\mathbf{H}\mathbf{H}^\dagger| \tag{5.0.1}$$

where $|.|$ denotes the matrix determinant, $\mathbf{I}_M$ is the $M \times M$ identity matrix and $\dagger$ signifies the conjugate transpose or Hermitian operation.

5.1 Flat fading Capacity Comparison

5.1.1 Uncorrelated Fading

For the $M \times M$ ULA, we know the asymptotic ergodic capacity as $M \to \infty$ is given by [39]

$$C_{ULA} = M \log_2(|1 + SNR|) \tag{5.1.1}$$

Similarly, the asymptotic capacity for the P-element MEA as $P \to \infty$ is given by

$$C_{MEA} = NP \log_2(|1 + SNR|) \tag{5.1.2}$$

It is evident that if $M = P$, the MEA offers a capacity gain factor of N bits/sec/Hz over the ULA for a given SNR, where N is constrained by the antenna radius a. For the $M = NP$ case both the ULA and the MEA will have equivalent capacity under the i.i.d Rayleigh fading assumption.

5.1.2 Correlated Fading

In the case of spatially correlated fading, the correlated MIMO channel $\mathbf{H}$ may be modeled as a product of transmit correlation matrix $\mathbf{R}_t$, a spatially white channel matrix $\mathbf{H}_w$ and a receive correlation matrix $\mathbf{R}_r$,

$$\mathbf{H} = \mathbf{R}_r^{1/2}\mathbf{H}_w\mathbf{R}_t^{1/2}. \tag{5.1.3}$$

The resulting MIMO capacity is defined as

$$C = \log_2(|\mathbf{I}_M + \frac{SNR}{M}\mathbf{R}_r^{1/2}\mathbf{H}_w\mathbf{R}_t\mathbf{H}_w^\dagger\mathbf{R}_r^{\dagger/2}|), \tag{5.1.4}$$

which is equivalent to the following at high SNR:

$$C \approx \log_2 |\frac{SNR}{M}\mathbf{H}_w\mathbf{H}_w^\dagger| + \log_2 |\mathbf{R}_r| + \log_2 |\mathbf{R}_t| \tag{5.1.5}$$

Assuming $M = NP$, i.e. $N = 1$ for a fair comparison, the received envelope correlation for both the ULA and MEA is given in [18], [10]. From 5.1.5 we obtain the result that the receive correlation for the MEA is higher than for the ULA, given $M = NP$.

It is trivial to check that for $M = P$ and $N > 1$ the MEA offers higher capacity even under correlated fading conditions.

5.2 Flat fading Diversity Comparison

5.2.1 No Channel State Information at Transmitter

For the $M \times M$ ULA, with the use of uncoded spatial multiplexing (independent data symbol transmission from each antenna) we can achieve an average Pairwise-Error-Probability (PEP) of

$$\overline{P}_{e,ULA} \leq \frac{1}{\lambda \mathbf{G}_{i,j}^M} \left(\frac{SNR}{4M}\right)^{-M} \tag{5.2.1}$$

The slope of the PEP curve shows that the achievable diversity order for the ULA is M.

Similarly, the $P \times P$ MEA of N-multimode antennas will offer a diversity order of PM if $M = P$. Therefore the diversity gain is increased by a factor of P by using a multimode array.

5.2.2 Complete Channel State Information at Transmitter

If complete CSIT is assumed for the MIMO system, then the optimal diversity and array gain may be extracted from the system. Following the analysis in [16], the average PEP expressions for the ULA and MEA are

$$\overline{P}_{e,ULA} \geq \overline{N_e} \left(\frac{SNRd_{min}^2}{4}\right)^{-M^2} \tag{5.2.2}$$

$$\overline{P}_{e,MEA} \geq \overline{N_e} \left(\frac{SNRd_{min}^2}{4}\right)^{-P^2M^2} \tag{5.2.3}$$

From the exponent of the PEP, we can see that the diversity order for the MEA with full CSIT is P^2 times greater than the ULA diversity order.

5.3 Joint Spatial-Modal Waterfilling

Considering the $M \times M$ ULA with complete CSIT, the conventional power-allocation strategy is known as the waterfilling (or waterpouring) algorithm [1]. Knowledge of the channel allows the transmitter to decompose it into the constituent sub-channels and allocate variable transmit power according to the sub-channel strengths (eigenvalues). If the rank of channel matrix $\mathbf{H}$ is assumed to be r_H, then the MIMO capacity achieved by waterfilling restricted to the spatial domain is

$$C = \max_{\sum_{i=1}^{r_H} \gamma_i = M} \sum_{i=1}^{r_H} \log_2 \left(1 + \frac{SNR\gamma_i}{M}\lambda_i\right), \tag{5.3.1}$$

where λ_i is the i^{th} eigenvalue of $\mathbf{H}_w\mathbf{H}_w^\dagger$, and γ_i is the power allocated to the i^{th} sub-channel given a total power constraint of M. We have seen that multimode antennas offer additional degrees of freedom by means of MIMO diversity. This can be exploited by performing *joint spatial-modal* waterfilling, provided that the transmitter has complete CSIT. For a MEA with $P = M$ antenna elements and N multimodes per antenna, the rank of the effective channel matrix $\mathbf{H}_{eff}$ is Nr_H assuming orthogonal modes. In other words, Nr_H sub-channels are now available for data transmission.

$$C = \max_{\sum_{i=1}^{Nr_H} \gamma_i = NM} \sum_{i=1}^{Nr_H} \log_2 \left(1 + \frac{SNR\gamma_i}{M}\lambda_i(\mathbf{H}_{eff}\mathbf{H}_{eff}^\dagger)\right), \tag{5.3.2}$$

Chapter 6

SIMULATION EVALUATIONS

Ergodic capacities and mean error probabilities are obtained by averaging over a minimum of 10000 channel realizations in this section. The following SCM parameters were chosen for the subsequent numerical evaluations using MATLAB:

Table 6.1: SCM System Parameters

Number of paths N	1,2,3 and 6
Subpaths per path M	20
MS velocity v	1 m/s

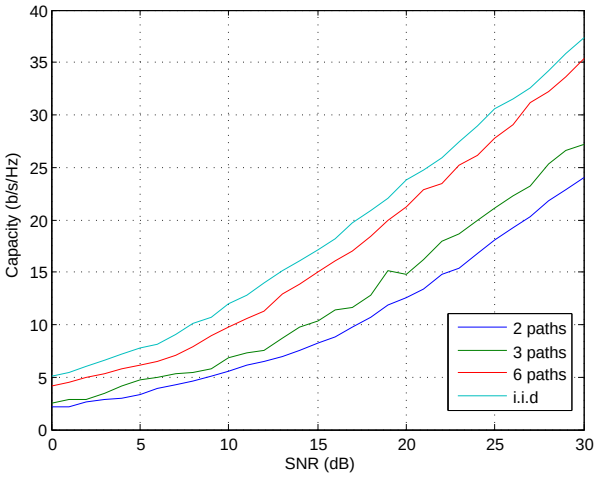

Figure 6.1: Multimode capacity versus SNR in flat-fading 3GPP urban micro-cell environment for $N_m = 6$ modes at both BS and MS, and N =2, 3 and 6 multipaths.

Fig. 6.1 is a compilation of 6-mode microstrip capacity performance versus SNR in

flat Rayleigh fading with 2, 3 and 6 multipaths in the SCM environment. As expected, system capacity increases with the richness of the multipath environment, for example the SCM with 6 scatterers enhances multimode throughput by 37.5% compared to 2 scatterers at 20 dB SNR.

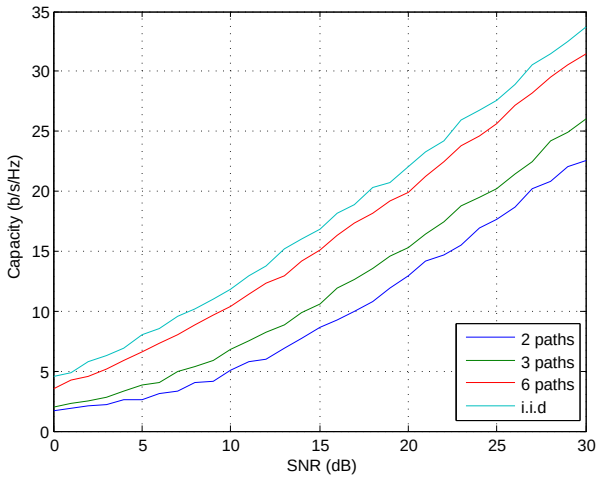

Figure 6.2: Throughput versus SNR in flat-fading 3GPP urban micro-cell environment for ULA with 6 dipoles at both BS and MS, and $N = 2$, 3 and 6 multipaths.

For comparison purposes, the capacity results are also obtained for a uniform linear array (ULA) of 6 dipoles at BS and MS operating in an identical 3GPP flat-fading SCM scenario as seen in Fig. 6.2. The 6 dipole ULA outperforms the multimode antenna with 6 modes by no more than 12% at any SNR value. The results for the multimode and ULA throughput in the 3GPP SCM show similar trends to the one-ring model capacity evaluation in [5].

Fig. 6.3 is a comparison of the throughput of a 6-mode microstrip and ULA with 5 and 6 dipoles versus SNR in a frequency-selective Rayleigh fading SCM environment with N = 6 multipaths. Once again the 6-dipole ULA outperforms the 6-mode microstrip e.g. by 15% at 25 dB SNR. However, the 6-mode patch is seen to offer consistently higher throughput than the 5-dipole ULA at all SNR values.

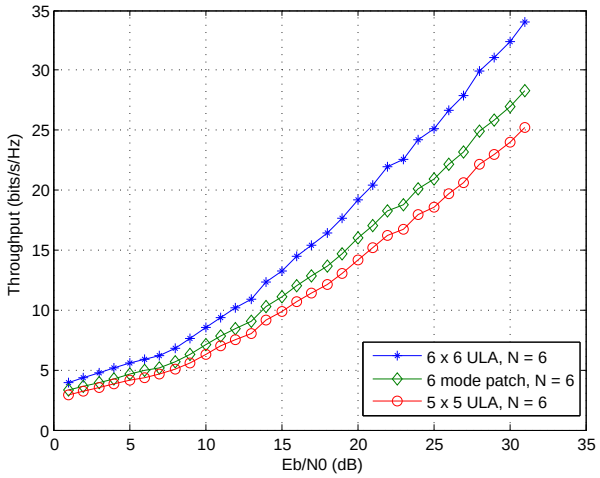

Figure 6.3: Throughput versus SNR in 3GPP urban micro-cell environment for ULA with 6 dipoles at both BS and MS, multimode patch with 6 modes, and ULA with 5 dipoles with frequency-selective fading.

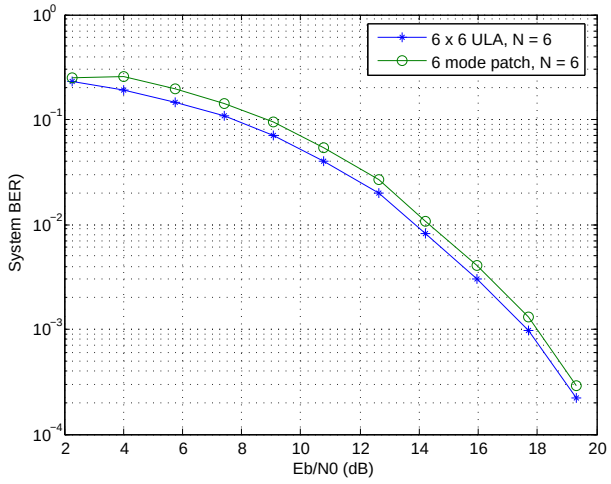

Figure 6.4: System BER versus SNR (dB) for frequency-domain ZF detection for 5 and 6-dipole ULA and 6-mode multimode antenna, adaptive MQAM modulation, frequency-selective fading channel.

Fig.6.4 displays the error performance of the 6-dipole ULA and 6-mode microstrip patch antenna respectively for ZF OFDM symbol equalization. It is observed that the 6-mode microstrip BER is within 0.9 dB of the 6-dipole ULA for all SNR values.

Tables 3 and 4 illustrate the improvement in multimode matched-filter detection by application of SPC. The detection of weaker modes is enhanced by 45% for mode $m = 1$, for example.

Table 6.2: Initial Spatial Matched Filter Stage Output, SNR = 5 dB

Mode1	Mode2	Mode3	Mode4	Mode5	Mode6
95	165	270	300	320	361

Table 6.3: Second Spatial Matched Filter Stage Output after SPC, SNR = 5 dB

Mode1	Mode2	Mode3	Mode4	Mode5	Mode6
173	282	290	313	360	0

Chapter 7

CONCLUSIONS

This paper demonstrates the feasibility of multiple-mode diversity using a single antenna in a realistic urban micro-cell environment for both flat and frequency-selective fading scenarios. A microstrip patch antenna employing up to 6 higher-order modes is found to be comparable to a conventional linear antenna array with a significantly lower cost in terms of size and spacing. The 3GPP SCM is modeled as the propagation environment to obtain pragmatic theoretical performance results that should be more compatible with experimental evaluations. Future research in this area may focus on combining spatial, frequency and multimode diversity, as well as a more thorough investigation on the optimal signal processing design for multimode antennas.

REFERENCES

List of References

[1] Emre Telatar, ”Capacity of multi-antenna Gaussian Channels,” *European Transactions on Telecommunications*, vol. 10, pp. 585-595, Nov./Dec. 1999.

[2] G. J. Foschini and M. J. Gans, ”On limits of wireless communication in a fading environment when using multiple antennas”, *Wireless Personal Communications*, vol. 6, no. 3, pp. 311-335, Mar. 1998.

[3] R. H. Clarke, ”A statistical theory of mobile radio reception, Bell. Syst. Tech. J., vol. 47, no. 6, pp. 957-1000, July/Aug. 1968.

[4] E. N. Gilbert, Energy reception for mobile radio, Bell Syst. Tech. J., vol. 44, pp. 1779-1803, 1965.

[5] P. Mattheijssen, M. A. J. Herben, Guido Dolmans, and L. Leyten, ”Antenna-Pattern Diversity Versus Space Diversity for Use at Handhelds,” *IEEE Transactions on Vehicular Technology*, vol. 53, pp. 1035-1042, July 2004.

[6] C. Degen and W. Keusgen, ”Performance evaluation of MIMO systems using dual-polarized antennas,” in *Proc. IEEE Global Telecommun*. Conf., Feb. 2003, vol. 2, pp. 1520-1525.

[7] T. Svantesson, ”On capacity and correlation of multi-antenna systems employing multiple polarizations,” in *Proc. IEEE Antennas & Propagation Symposium*, vol. 3, pp. 202-205, Jun. 2002.

[8] F. Demmerle and W. Wiesbeck, ”A biconical multibeam antenna for space-division multiple access,” *IEEE Transactions on Antennas and Propagation*, vol. 46, no. 6, pp. 782-787, 1998.

[9] C.Waldschmidt and W. Wiesbeck, ”Compact Wide-Band Multimode Antennas for MIMO and Diversity,” *IEEE Transactions on Antennas and Propagation*, vol. 52, no. 8, pp. 1963-1970, August 2004.

[10] T. Svantesson, ”Correlation and channel capacity of MIMO systems employing multimode antennas,” *IEEE Transactions on Vehicular Technology*, vol. 51, pp. 1304-1311, Nov 2002.

[11] Forenza and R. Heath,” Benefit of Pattern Diversity via Two-Element Array of Circular Patch Antennas in Indoor Clustered MIMO Channels,” *IEEE Transactions on Communications*, vol. 54, pp. 943-954, May 2006.

[12] R. G. Vaughan, ”Two-port higher mode circular microstrip antennas,” *IEEE Transactions on Antennas and Propagation*, vol. 36, pp. 309-321, Mar. 1988.

[13] W. C.Jakes, *Microwave Mobile Communications*, New York: IEEE Press, 1993.

[14] J. H. Winters, ”On the capacity of radio communication systems with diversity in a rayleigh fading environment,” *IEEE Journal on Selected Areas in Communications*, vol. 5, pp. 871-877, May 1987.

[15] F. Molisch, M. Steinbauer, M. Toeltsch, E. Bonek, and R. S. Thoma, ”Capacity of MIMO systems based on measured wireless channels,” *IEEE Journal on Selected Areas in Communications*, vol. 20, pp. 561-569, April 2002.

[16] David Gesbert, Helmut Blcskei, Dhananjay A. Gore and Arogyaswami J. Paulraj, ”Outdoor MIMO Wireless Channels: Models and Performance Prediction,” *IEEE Transactions on Communications*, vol. 50, no. 12, pp. 1926-1935, Dec. 2002.

[17] R. Janaswamy, ”Effect of Element Mutual Coupling on the Capacity of Fixed Length Linear Arrays,” *IEEE Antennas and Propagation Letters*, vol. 1, pp. 157-161, 2002.

[18] K. I. Pedersen, P. E. Mogensen, and B. H. Fleury, ”Spatial channel characteristics in outdoor environments and their impact on BS antenna system performance,” in *Proc. 48th IEEE VTC*, vol. 2, pp. 719723, May 1998.

[19] D. Y. Yacoub, C. Schneider, S. Warzuegel, W. G. Teich, R. Thom, J. Lindner, ”Capacity of Measured MIMO Channels in Dependence of Array Element Spacing and Distance between Antennas,” in Proc. of International ITG / IEEE Workshop on Smart Antennas, 2006.

[20] M. Herdin, M. Gritsch, G. Badic, E. B. Bonek, ”The influence of channel models on simulated MIMO performance,” in *Proc. IEEE VTC* Milan, Spring, 2004.

[21] D.S. Shiu, G. J. Foschini, M. J. Gans, J. M. Kahn, “Fading correlation and its effect on the capacity of multielement antenna systems,” *IEEE Transactions on Communications*, vol. 48, pp. 502513, Mar. 2000.

[22] 3rd Generation Partnership Project (3GPP), ”Spatial channel model for multiple input multiple output (MIMO) simulations (3gpp tr 25.996 version 6.1.0 release 6),” ETSI, Tech. Rep., 2003.

[23] R. Garg, P. Bhartia, I. Bahl, and A. Ittipiboon, *Microstrip Antenna Design Handbook*: Artech House, 2001.

[24] C. Balanis, *Antenna Theory Analysis and Design*, John Wiley & Sons, Inc., 1982.

[25] C. Wong et al, ”Multiuser OFDM with Adaptive Subcarrier, Bit, and Power Allocation”, *IEEE Journal on Selected Areas in Communications*, Vol. 17, No. 10, pp. 1747-1758, October 1999.

[26] A.J. Goldsmith and S.G. Chua, ”Variable-Rate Variable-power MQAM for. Fading Channels”, *IEEE Transactions on Communications*, vol. 45, no. 10, pp. 1218-1230, Oct. 1997.

[27] S. M. Kay, *Fundamentals of Statistical Signal Processing: Estimation Theory*, Prentice Hall, 1993.

[28] J. Proakis, Digital Communications, McGraw-Hill, 4 ed. , 2001.

[29] J. F. Valenzuela-Valdes, M. Garcia-Fernandez, A. Martinez-Gonzalez, D. Sanchez-Hernandez, ”The role of polarization diversity for MIMO systems under Rayleigh-fading environments,”*Antennas and Wireless Propagation Letters*, pp. 534-536, Dec. 2006.

[30] T. L. Marzetta, ”Fundamental limitations on the capacity of wireless links that use polarimetric antenna arrays,” in *Proc. of International Symposium on Information Theory* 2002, p. 51, July 2002.

[31] J.Walfisch and H.L. Bertoni, ”A Theoretical model of UHF propagation in urban environments,” *IEEE Transactions on Antennas and Propagation*, vol. 36, pp. 1788-1796, 1988.

[32] F.Ikegami, T.Takeuchi, and S.Yoshida, ”Theoretical prediction of mean field strength for Urban Mobile Radio”, *IEEE Transactions on Antennas and Propagation*, Vol.39, No.3, 1991.

[33] Har D., Watson, A.M.,and Chadney, A.G., ”Comment on Diffraction Loss of Rooftop to-Street in COST 231-Walfisch-Ikegami Model”, *IEEE Transactions on Vehicular Technology*, vol.48, no.5, pp. 1451-1452, 1999.

[34] J. Medbo, D. Browne and H. Asplund, ”MIMO ChannelMeasurements in an Urban Microcell,” in *Proc. of RadioVetenskap och Kommunikation*, Stockholm, Sweden, June 2002.

[35] Cheng-Xiang Wang, Xuemin Hong, Hanguang Wu, and Wen Xu,”Spatial Temporal Correlation Properties of the 3GPP Spatial Channel Model and the Kronecker MIMO Channel Model,” to appear, *Eurasip Journal On Wireless Communications and Networking*, 2007.

[36] T.C.W. Schenk, R.J.C. Bultitude, L.M. Augustin, R.H. van Poppel and G. Brussaard, ”Analysis of Propagation Loss In Urban Microcells at 1.9 GHz and 5.8 GHz,” in Proc. URSI Commission F Open Symposium on Radiowave Propagation and Remote Sensing,Germany, February 12-15, 2002.

[37] P.G. Brown and C.C. Constantinou, ”Investigations on the prediction of radiowave propagation in urban microcell environments using ray-tracing methods,” *IEE Proceedings - Microwaves, Antennas and Propagation*, February 1996, Volume 143, Issue 1, p. 36-42.

[38] G. G. Raleigh and J. Cioffi, ”Spatio-Temporal Coding for Wireless Communication,” *IEEE Transactions on Communications*, vol. 46, no. 3, pp. 357-367, Mar. 1998.

[39] Paulraj, R. Nabar and D. Gore, *Introduction to Space-Time Wireless Communications*, Cambridge University Press 2003.

[40] P. Almers,F. Tufvesson, O. Edfors, and A. Molisch, ”Measured capacity gain using water filling in frequency selective MIMO channels,” in *Proc. of 13th Personal, Indoor and Mobile Radio Communications*, pp. 1347-1351, 2002.

[41] H. Blocskei, D. Gesbert and A. Paulraj, ”On the Capacity of OFDM-Based Spatial Multiplexing Systems,” *IEEE Transactions on Communications*, vol. 50, no. 2, pp. 225-234, Feb. 2002.

[42] L. Cimini, ”Analysis and Simulation of a Digital Mobile Channel Using Orthogonal Frequency Division Multiplexing,” *IEEE Transactions on Communications*, vol. 33, no. 7, pp. 665-675, July 1985.

[43] P. Petrust, J. H. Reed, and T. S. Rappaport, ”Geometrically based statistical channel model for macrocellular mobile environments,” in *Proc. of IEEE Global Telecommunications Conference*, vol. 2, pp. 11971210, Nov. 1996.